Nystagmus in the B6(CG)Tyr(c-2J)/J Albino Mouse: A Functional and RNA-Seq Analysis

Laura L. Johnson,[1,2] Juan E. Abrahante,[3] and Linda K. McLoon[1,2]

[1]Department of Ophthalmology and Visual Neurosciences, University of Minnesota, Minneapolis, Minnesota, United States
[2]Graduate Program in Cellular, Molecular, Developmental Biology and Genetics, University of Minnesota, Minneapolis, Minnesota, United States
[3]University of Minnesota Informatics Institute, University of Minnesota, Minneapolis, Minnesota, United States

Correspondence: Linda K. McLoon, Department of Ophthalmology and Visual Neurosciences, University of Minnesota, Room 374 Lions Research Building, 2001 6th Street SE, Minneapolis, MN 55455, USA; mcloo001@umn.edu.

Received: July 24, 2023
Accepted: December 26, 2023
Published: January 11, 2024

Citation: Johnson LL, Abrahante JE, McLoon LK. Nystagmus in the B6(CG)Tyr(c-2J)/J albino mouse: A functional and RNA-Seq analysis. *Invest Ophthalmol Vis Sci.* 2024;65(1):26. https://doi.org/10.1167/iovs.65.1.26

Purpose. Infantile nystagmus syndrome (INS) is a gaze-holding disorder characterized by conjugate, uncontrolled eye oscillations that can result in significant visual acuity loss. INS is often associated with albinism, but the mechanism is unclear. Albino mice have nystagmus; however, a pigmented mouse with a *tyr* mutation making it phenotypically albino, the B6(CG)-Tyr(c-2J)/J (B6 albino), had not been tested. We tested optokinetic response (OKR) in B6 albino and control mice. RNA-Seq was performed on extraocular muscles (EOM), tibialis anterior (TA) muscle, abducens (CN6), and oculomotor (CN3) neurons to uncover molecular differences that may contribute to nystagmus.

Methods. OKR was measured using an ISCAN system. RNA was isolated from four tissues to identify differentially expressed genes and validated with qPCR and immunohistochemistry. Ingenuity pathway analyses identified top biological pathways.

Results. All B6 albino mice tested had nystagmus. Differential RNA expression analysis showed 383 genes differentially expressed in EOM, 70 in CN3, 20 in CN6, and 639 in the TA. Two genes were differentially expressed in all four tissues: *wdfy1* and *nnt*. Differences were validated by qPCR and immunostaining.

Conclusions. The *tyr* mutation in B6 albino mice, genotypically pigmented and phenotypically albino, is sufficient to result in spontaneous nystagmus. The two genes with decreased expression in the B6 albino tissues examined, w*dfy1* and *nnt*, have been implicated in mitochondrial dysfunction and stem cell maintenance in other systems. Their function in extraocular muscle is unknown. These studies suggest that this mouse model of nystagmus may allow molecular identification of candidate nystagmus-related genes.

Keywords: extraocular muscles, nystagmus, RNA-seq, gene expression, albinism

Infantile nystagmus syndrome (INS) is a gaze holding disorder characterized by uncontrollable oscillations of the eyes. In the case of INS, patients will present with these oscillations before the age of 6 months.[1] A large number of cases of INS are idiopathic and have no known cause associated with the disorder. INS is commonly associated with sensory afferent defects, such as optic nerve hypoplasia or albinism.[2] There are a number of genetic mutations that cause albinism in humans, and many of these individuals also have infantile nystagmus. Generally the oscillation frequency of these human individuals with nystagmus varies between 0.5 to 8 hertz.[3] Mutations have been described in the following genes, and they all result in hypopigmentation of the eyes: OCA1/2/3/4, TYR, TYRP1, and MATP.[4] The prevalence of albinism and infantile nystagmus together is roughly 2.5 per 10,000 in humans.[1]

Albino mice are an excellent animal model for the study of infantile nystagmus.[5] Traber et al.[5] measured optokinetic reflexes (OKR) in the dark and in the presence of an optokinetic stimulus. They showed that in albino (BALB/C and CD1) and in hypo-pigmented mice (DBA1), spontaneous eye movements were seen in the dark, and all showed nystagmus-like waveforms in the presence of the optokinetic stimulus.[5] C57BL/6 mice had normal OKR in the presence of the optokinetic stimulus.

A developed mouse strain, B6(CG)-Tyr(c-2J)/J that we refer to as B6 albino, is genetically identical to a C57BL/6 mouse, but with a mutation in the tyrosinase gene, *tyr*, making this mouse phenotypically albino. This mouse has pigment completely absent from skin, hair, and eyes and does not have the genetic variances that other albino strains have compared to the pigmented C57BL/6 mouse, making it an excellent candidate to use as a nystagmus model.[6] The extraocular muscles (EOM) and the eye movements of this mouse were not previously studied.

Eye movements are studied using eye tracking systems in humans as well as animal models. Specifically, we can examine the OKR waveforms in both humans and animal models. The OKR consists of tracking the movements of the eyes in response to a stimulus of moving black and white bars in the horizontal or vertical plane. The eyes move in a very stereotypical manner, because this is a reflex, and

reproducible movements of the eyes can be tracked using video cameras focused on the eyes. In mice, recording of OKR movements requires that the head be stabilized and using a video camera, we can record eye movements in the presence or absence of the stimulus that produces the OKR.

We hypothesize that the B6 albinos will have eye movement waveforms consistent with INS, as compared to control C57BL/6 mice, which will have normal eye movements. We further hypothesize that an analysis of the transcriptome of the EOM and blocks of oculomotor (CN3) and abducens motor neurons (CN6) from each mouse genotype could illuminate genes differentially expressed between the B6 albino mice in the absence of the stimulus that produces the OKR and the control pigmented mice that might be related to the onset or maintenance of these abnormal eye movements. Tibialis anterior (TA) muscles provided us with a way to eliminate nerve- and muscle-specific genes that were not related to eye movements. These analyses generated a number of candidate molecules and pathways that may be involved in some cases of idiopathic INS in humans.

Methods

Animals

C57BL/6 and B6(Cg)-*Tyr*$^{c-2J}$/J (B6 albino) mice were obtained from Jackson Laboratory (Bar Harbor, ME, USA) and housed with Resource Animal Resources at the University of Minnesota with 12 hour light/dark cycle and food ad libitum. All animal studies followed the guidelines of the National Institutes of Health and the Association for Research in Vision and Ophthalmology, and all experiments were approved by the Institutional Animal Care and Use Committee at the University of Minnesota.

OKR Testing

OKR was assessed as described previously.[7] In preparation for measurement of OKR, head posts were implanted to stabilize the head during testing. After a sterile incision was made into the scalp, the skull was cleaned, and head-posts were implanted by first inserting 000 × 3/32" self-tapping screws into the mouse skull on the top of the head. Geristore dental cement (DenMat LLC, Lompoc, CA, USA) was placed on top of the screws and surrounding skull area to create a cap in which to insert the head-posts. M3 × 0.5 mm nylon pan head slotted screws, with the screw heads removed, were placed vertically into the Geristore cement before it dried; this created posts on the mouse head for stabilization during pupil tracking experiments. Mice were allowed to recover from surgery for two weeks before testing. OKR traces were performed on a total of 18 C57BL/6 mice and 31 B6 albino mice.

Once mice recovered from head-post surgery, and before testing began, they were placed in a dark room for at least 12 hours to acclimate to the dark. A number of previous studies had been unable to record eye movements in albino mice of various strains (CD1[8]; BALB/c[9]; DBA2[9,10]), despite the presence of normal structure and function of the retina itself.[9] The retinas of these mice appeared to be normal. Photophobia is present in these mice[8]; thus it is not surprising that dark adaptation allows for eye movements to be recorded when using OKR. The ISCAN program (ISCAN, Inc. Woburn, MA) used for tracking eyes cannot distinguish an albino mouse's pupil; therefore, if a mouse was albino, a small temporary tattoo was placed on the mouse's cornea to represent the pupil for detection by the program. This was previously shown to be an accurate alternative to pupil tracking.[11] The C57BL/6 mice used as controls had their pupil detected by the program without a tattoo. The tattoo was created using a mixture of iron oxide and H_2O, then placed onto the eye lateral to the pupil using a blunted needle. No signs of corneal edema occurred in any of these albino mice. Normal eye blinks remove the tattoo after about 45 minutes. After the tattoo was placed, the mouse's eye movements were recorded while still in the dark room, immobilized using a clamp attached to the head-posts and a tube around their bodies. During testing, the mice were surrounded by a white circular drum with black bars projected onto the white background. The stimulus velocity was 0.5 cycles/second for all testing, and horizontal and vertical eye movements were recorded. Each mouse was testing using a series of optokinetic stimuli with Michelson contrasts of 10, 25, 50, 75, 100, 200, and 400 and a series of optokinetic stimuli at 0.06, 0.08, 0.10, 0.12, and 0.15 cycles/deg. After a period of rest, pupil tracking was performed in the absence of the optokinetic stimulus. These series were not randomized, so that each mouse followed the same pattern of contrast variations and differing spatial frequencies. Graphs were generated of the full 86 seconds and then processed further to show 20 second segments of each trace to remove tracings where there were a lot of eye blinks or loss of ability to track the tattoo by the video camera momentarily. The black bars moved left to right across the mouse's vision field with the above delineated sequences of spatial frequencies and varying contrasts for a total of 86 seconds, and eye movements tracking these rotating bars were recorded using a camera and the ISCAN program. The ISCAN program measures horizontal and vertical components of the movements of the mouse's pupil or eye tattoo (named the pupil trace), and using a corneal reflection created by a red light near the camera aimed on the mouse eye. Calibration for each mouse was done prior to recording eye movements using both no stimuli and stimuli in the ISCAN program to set the detection of the pupil or eye tattoo and the corneal reflection. To analyze the data from the ISCAN program, raw files of horizontal and vertical movement components were uploaded into a custom program in R (R Foundation for Statistical Computing, Vienna, Austria), where the raw pupil trace was filtered by subtracting the raw corneal reflection trace to remove extra head movements. The average horizontal and vertical positions were calculated for each trace, with each set arbitrarily at zero and −20, respectively, for ease of graphic representation. OKR responses were characterized based on published waveform analyses.[12]

RNA-Seq

RNA was isolated from the following tissues: EOM, TA, a block containing abducens cranial motor neurons (CN6), and a block containing the oculomotor cranial motor neurons (CN3) from four mice per genotype. An RNA-Seq dataset was compiled using tissue obtained from four C57BL/6 and four B6 albino mice. The EOM, the TA, a block containing the CN6 neurons and a block containing the CN3 neurons were dissected from each mouse. EOM, TA, CN6, and CN3 tissues were prepared for RNA-Seq using either the RNeasy Fibrous Tissue Mini Kit (Qiagen, Germantown, MD, USA) or RNeasy Lipid Tissue Mini Kit (Qiagen). After isolation, RNA was assessed for quality using RNA Integrity Number score as assayed

using an Agilent 2100 Analyzer. The cutoff point for the RNA Integrity Number score was 8. These analyses were performed by University of Minnesota Genomic Core facility. RNA-Seq was performed by the University of Minnesota Genomics Center, and all samples were run on a HiSeq 2500 (Illumina, San Diego, CA, USA) instrument. The University of Minnesota Informatics Institute analyzed the RNA Seq output. 2 × 150bp FastQ paired-end reads for 32 samples (n = 22.3 million average per sample) were trimmed using Trimmomatic (v 0.33) enabled with the optional "-q" option; 3bp sliding-window trimming from 3′ end requiring minimum Q30.

Quality control on raw sequence data for each sample was performed with FastQC. Read mapping was performed via Hisat2 (v2.1.0) using the mouse genome (mm10) as a reference. Gene quantification was done via Feature Counts for raw read counts. Differentially expressed genes were identified using the edgeR (negative binomial) feature in CLCGWB (Qiagen) using raw read counts.

Genes were qualified as differentially expressed in the varying tissue types (EOM, TA, CN3, and CN6) between the B6 albino mice and the C57BL/6 mice by having a minimum 2x Absolute Fold Change and a corrected P value < 0.05.

Principal component analysis (PCA) plots were generated along with a heat map comparing the different samples from all the tissue types in the B6 albino mice and the C57BL/6 mice to visually validate the RNA-Seq data. Gene plots on log2 transformed CPM values were generated for visualizing different RNA levels of the two genes between the B6 albino mice and the C57BL/6 mice for each tissue. Venny[13] tools were used to numerically visualize genes differentially expressed in multiple tissues.

Differentially expressed gene datasets were uploaded into Ingenuity Pathway Analysis (IPA) (Qiagen) for pathway and functional analysis. Pathways for the EOM and TA were analyzed by IPA groups: cellular growth, proliferation and development, and organismal growth and development. Each tissue type was also analyzed for physiological system development and function through IPA. Graphs were displayed using −log (P value), with the threshold set at P value = 0.05. All data are deposited in GEO and can be found using this accession number: acc = GSE245207.

Gene Validation

Genes that were found differentially expressed were validated or confirmed using qPCR. The EOM, the TA, a block containing the CN6 neurons and a block containing the CN3 neurons were dissected from each mouse. These tissues were prepped using Qiagen Tissue Ruptor, and then RNA was isolated using either the RNeasy Fibrous Tissue Mini Kit (Qiagen) or RNeasy Lipid Tissue Mini Kit (Qiagen). cDNA was constructed from the isolated RNA using the Transcriptor First Strand cDNA Synthesis Kit (Roche, Basel Switzerland). Primers were designed using PrimerBLAST (NCBI) and synthesized by IDT (Integrated DNA Technologies, Coralville, IA, USA). Samples were prepped for qPCR using Fast Start Essential DNA Green Master (Roche) and run on a LightCycler 96 System (Roche).

Immunohistochemistry

Adult B6 albino and control mice (N = 4 per genotype) were euthanized with an overdose of carbon dioxide using a tank system. The eyes with all rectus muscles attached were removed, embedded in tragacanth gum, and frozen in 2-methylbutane on liquid nitrogen, sectioned at 12 µm, and placed in a −30°C freezer for storage. For immunostaining, cryosections were rinsed in PBS, and blocked with 20% goat serum containing 0.2% bovine serum albumin in antibody buffer (PBS containing 0.2% Triton-X-100) for 30 minutes. This was followed by incubation with a rabbit antibody to WDFY1 (1:50 in antibody buffer; cat. LS-B12648; LifeSpan Biosciences, Shirley, MA, USA) for one hour at room temperature. After a rinse in PBS, the sections were blocked with 20% goat serum containing 0.2% bovine serum albumin in antibody buffer (PBS containing 0.2% Triton-X-100) for 30 minutes, followed by incubation with goat-anti-rabbit IgG AF488 (1:100, cat. 111-545-144; Jackson ImmunoResearch, West Grove, PA, USA) for 30 minutes. This process was repeated with incubation in a mouse primary antibody against embryonic (1:20, BF-45; Developmental Hybridoma Bank, Ames, IA, USA) or type IIX myosin heavy chain (MyHC) isoform (1:20, BF-35; Developmental Hybridoma Bank) for one hour at room temperature followed by incubation with a goat anti-mouse IgG DyLight 405 antibody (1:100, cat. 115-475-146; Jackson ImmunoResearch) for 30 minutes. After a PBS rinse, the slides were coverslipped using Vectashield antifade mounting medium (H-1700; Vector Laboratories, Burlingame, CA, USA). Slides were photographed using a Leica DM4000B fluorescence microscope (Leica, Wetzlar, Germany). Numbers of myofibers positive for a specific protein were analyzed and presented as a percent of total fibers. Four sections from four mice of each genotype were used for WDFY1 and IIA MyHC isoform coexpression analysis. A minimum of 200 myofibers were counted in each section for the EOM, in each layer, and these were averaged for each mouse. Significant differences were determined using GraphPad Prism 10.0 software (GraphPad, San Diego, CA, USA) using unpaired t-tests, where $P < 0.05$. F-tests were run to determine normal variance on the data.

Results

Effects of the Tyr Mutation on EOM Function

Extraocular muscle function was tested using the OKR. In the pigmented C57BL/6 mice for all ages tested, the OKR were normal (Figs. 1A, 1B). In the absence of stimuli, the eyes were relatively motionless in the C57BL/6 mice except for an occasional saccade (Fig. 1A). In the same pigmented mice, the presence of the OKR stimulus across the mouse's field of vision resulted in normal slow and fast phase responses characteristic of normal OKR (Fig. 1B).

In the unpigmented B6 albino mice, abnormal spontaneous eye movements were present in the absence of visual stimuli (Figs. 1C, 1E, 1G, 1I). Some of these mice had pendular waveforms (Figs. 1E, 1G), whereas others showed jerk nystagmus (Fig. 1I) or reverse slow and fast phase movements (Fig. 1C). In the presence of the OKR stimuli, the unpigmented B6 albino mice had abnormal and erratic eye movements that resembled the spontaneous eye movements in the absence of the OKR stimulus seen in human individuals with albinism and nystagmus (Figs. 1D, 1F, 1H, 1J).[14] Most of these erratic and oscillatory eye movements were pendular waveforms, with occasional jerks (Figs. 1D, 1F, 1H). Although there were a small number of similarities between the B6 albino mouse eye oscillations during no stimuli and stimuli testing (Figs. 1E, 1F), all showed abnormal and erratic eye oscillations frequencies that ranged between 0.2 to 1 Hz.

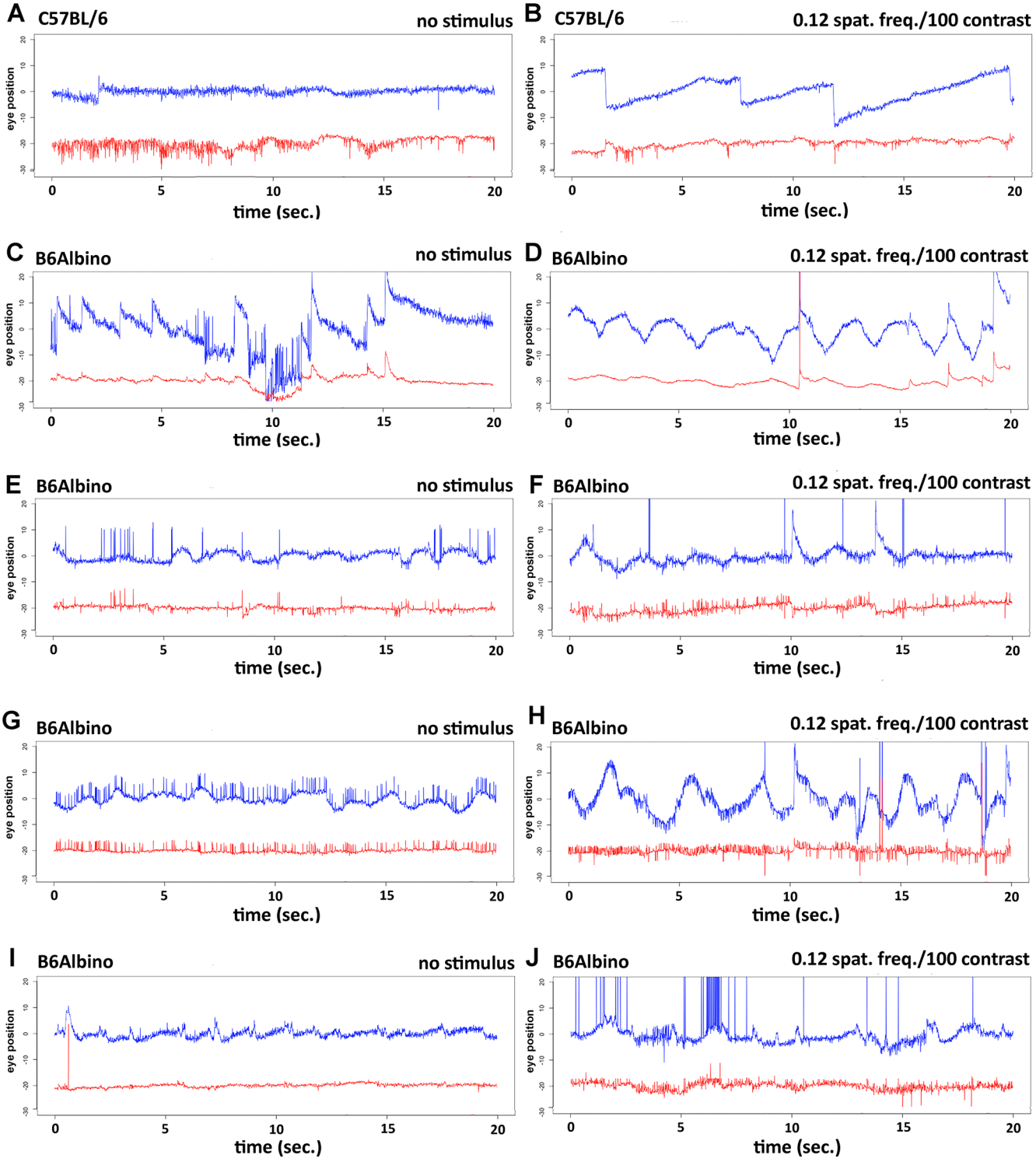

Figure 1. OKR responses for C57BL/6 (N = 18) compared with B6(CG)-Tyr$^{(C\text{-}2J)}$/J (B6 albino) (N = 31) mice. The graphs show eye position in horizontal (*blue line*) and vertical (*red line*) components as a function of time for 20 seconds. OKR was recorded using an ISCAN device. Eye movements were analyzed using a video camera to capture movements during no stimuli and during stimuli of moving black bars on a white background with a spatial frequency of 0.12 and a contrast of 100. C57BL/6 mice were used as a control and exhibited normal OKR during no stimuli (**A**) and stimuli (**B**) compared with B6 albino mice with differing waveforms of nystagmus during both no stimuli (**C**, **E**, **G**, **I**) and stimuli (**D**, **F**, **H**, **J**) measurements. No vertical nystagmus was seen. Random vertical spikes represent eyeblinks or momentary loss of the tattoo or pupil by the video camera.

Investigative Ophthalmology & Visual Science

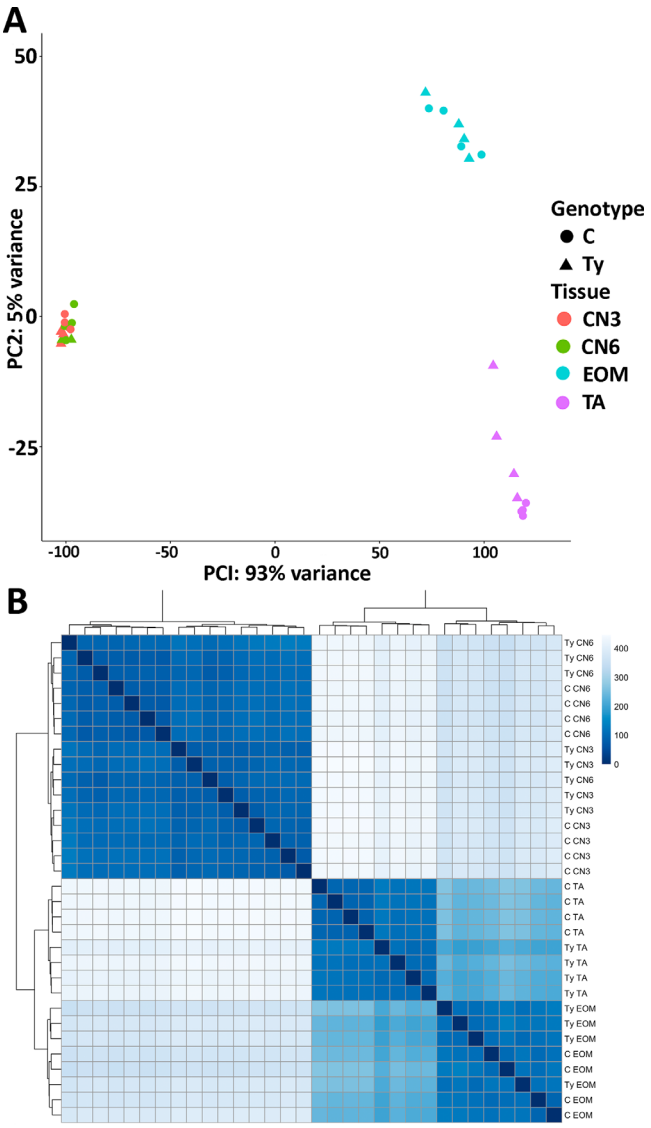

Figure 2. (**A**) PCA plot analyzing samples from the RNA-Seq experiment. This was created using the DESeq2 package in R to analyze the first principal components across samples from the RNA sequences performed. C = C57BL/6 mice in *circles*, Ty = B6 albino mice in *triangles*. CN3 and CN6 for both C57BL/6 and B6 albinos clustered tightly together. EOM and TA for both C57BL/6 and B6 albinos clustered together on the first principal component, but separated by tissue on the second principal component. (**B**) Heat map of sample-to-sample distances analyzing samples from the RNA-Seq experiment. This was created using the DESeq2 package in R to analyze which samples were similar to each other by gene expression. C, C57BL/6 mice; Ty, B6 albino mice. CN3 and CN6 for both C57BL/6 and B6 albinos express genes similar to each other. EOM and TA for both C57BL/6 and B6 albinos also express similar genes to each other, less closely than the CNs, shown by the color gradient.

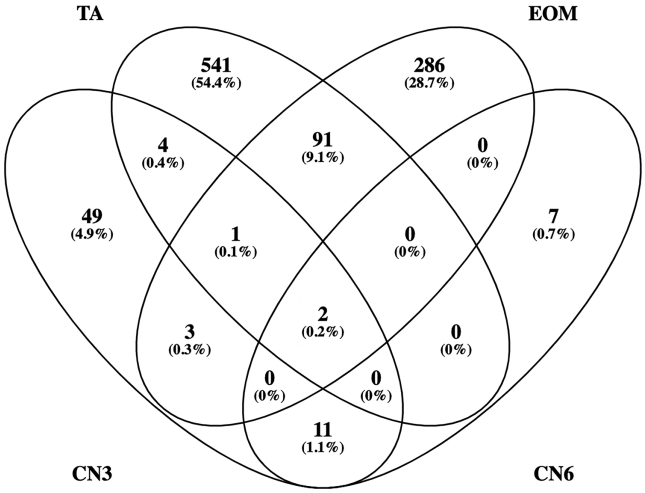

Figure 3. Venn diagram of differentially expressed genes between the C57BL/6 and B6 albino mice in each tissue type. Created using Venny (Juan Carlos Oliveros, Venny 2.1). Differentially expressed genes between the two genotypes in each tissue were compared to the other tissues and grouped in a Venn diagram format to showcase genes differentially expressed in multiple tissue types. There are two genes that are differentially expressed in all four of the tissue types.

Analysis of Differentially Expressed Genes

Differentially expressed genes are displayed in the neurons from CN3, neurons from CN6, the EOM, and the TA muscles of the B6 albino mice and the C57BL/6 mice. Four samples of each tissue from each mouse were used in this analysis. When examining the comparison across all 32 of the samples, a PCA plot was used to look at sample-wide differences (Fig. 2A). PCA plots were used to reduce the dimensionality of large sample sets such as an RNA-Seq dataset. The first principal component between samples divided them into groups that reflected tissue type: one group was the cranial motor neurons (CN3 and CN6), the others were the two muscle tissues (EOM and TA). The second principal component between samples broke the two muscle sample groups into two, EOM and TA, but kept the cranial motor neuron group in close proximity. This is most likely due to the EOM being developmentally and morphologically different from other limb or skeletal muscles such as the TA. Next, a heat map using sample-to-sample distances of all 32 samples showed similarities across samples in relation to each other (Fig. 2B). The heat map showed that the cranial motor neurons had very similar gene expression profiles to each other. The EOM and TA had similar profiles to each other, but less so than the gene expression profiles of the two groups of cranial motor neurons.

When looking at the differentially expressed genes between the C57BL/6 and the B6 albino mice, there were a total of 383 genes differentially expressed in the EOM, 70 in the CN3 neurons, 20 in the CN6 neurons, and 639 in the TA (Supplemental Table S1). The TA allowed us to eliminate genes under the assumption that they would not be involved in eye movement function. The number of overlapping genes differentially expressed between each tissue was plotted using Venny[8] (Fig. 3). When examined based on comparisons within tissue types, there were 286 differentially expressed genes in only the EOM between genotypes, 49 only in the CN3 neurons, seven only in the CN6 neurons, and 541 only in the TA (Supplemental Table S2). Ninety-one genes differentially expressed in both the EOM and TA, 11 genes differentially expressed in CN3 and CN6, four genes in both the TA and CN3, three genes in both the EOM and CN3, and one gene in the TA, EOM, and CN3 (Supplemental Table S3). There are two genes that are differentially expressed in each of the four tissue types between the C57BL/6 and the B6 albino mice, *nnt* and *wdfy*. Both were downregulated in the B6 albino compared to the

Investigative Ophthalmology & Visual Science

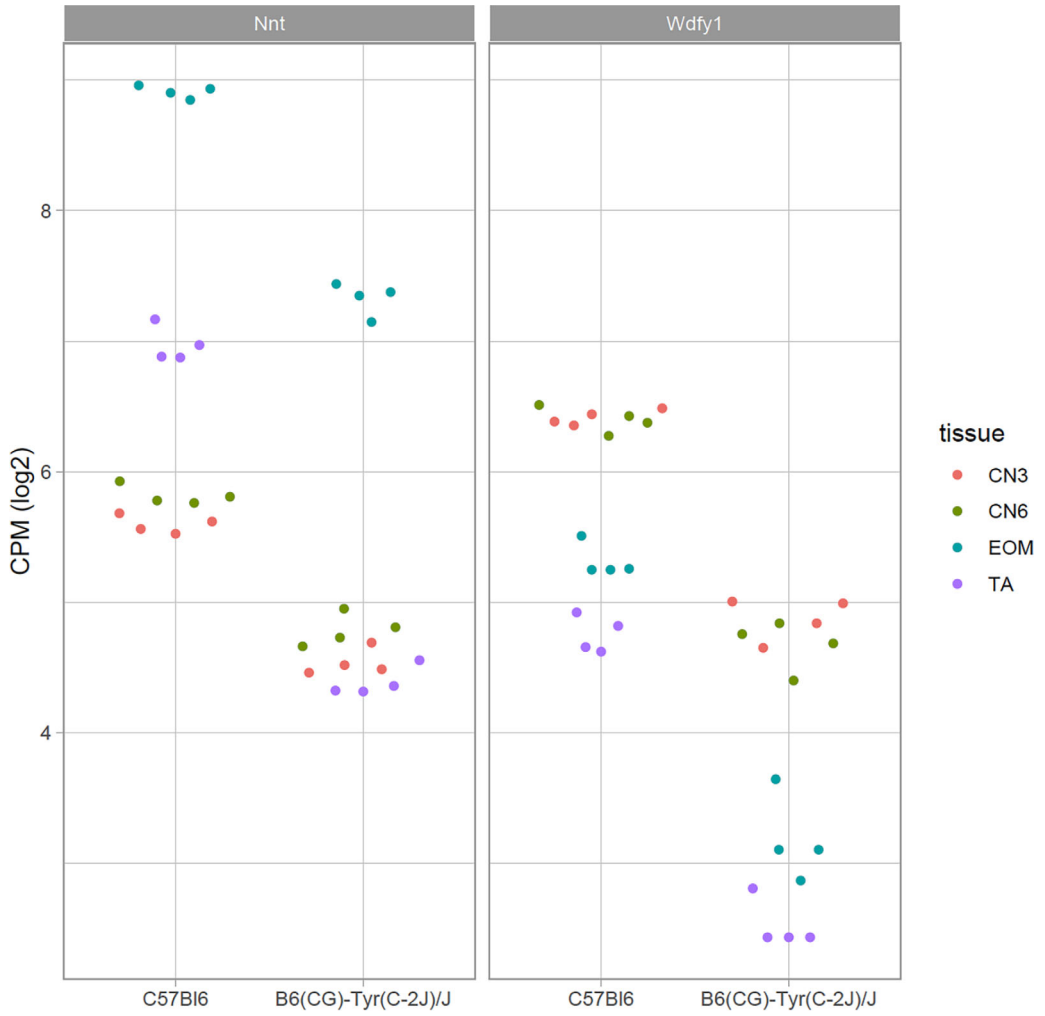

Figure 4. Gene count plot for *nnt* gene expression in C57BL/6 and B6 albino mice across all tissues. Each point represents a single sample from each genotype and each tissue, 32 samples in total. Please note that the y-axis representing the gene count data is a log scale. These were created using DESeq2 package in R. Count data in log scale. *Nnt* RNA expression is down in the B6 albinos compared to the C57BL/6 mice in every tissue type listed. Gene count plot for *wdfy1* gene expression in C57BL/6 and B6 albino mice across all tissues were created using DESeq2 package in R. Count data in log scale. *Wdfy1* RNA expression is down in the B6 albinos compared to the C57BL/6 mice in every tissue type listed.

C57BL/6 in all four tissues analyzed (Fig. 3; Supplemental Table S3).

Gene count plots were generated for both genes, *nnt* and *wdfy1,* which were differentially expressed in all of the tissue types (Fig. 4). All four of the tissue types had both *nnt* and *wdfy1* down-regulated in the B6 albino compared to the C57BL/6.

PCR Validation of the Identified Differentially Expressed Genes

The differential expression of these two genes was validated using qPCR, which confirmed that both the *wdfy1* and the *nnt* genes were significantly down-regulated in the B6 albino compared to the C57BL/6 in both the EOM and the TA, with decreases of 85.7% for EOM ($P = 0.0032$) and 86.5% for TA ($P = 0.0001$) (Figs. 5A, 5B). The *nnt* genes were significantly down-regulated in both the B6 albino EOM and TA compared to the C57BL/6, with decreases of 88.5% ($P = 0.035$) and 88.3% ($P = 0.0001$), respectively (Figs. 5C, 5D).

Immunofluorescence Validation of the Identified Differentially Expressed Genes

Further validation of the RNA-seq analysis was performed by immunostaining for WDFY1 and embryonic MyHC isoform expression on extraocular muscle sections from B6 albino and C57BL/6 mice (Fig. 6). Immunostaining of WDFYI in the B6 albino extraocular muscle was decreased compared to the control mouse EOM, confirming the differential expression seen in the RNA-Seq data. We examined the EOM for coexpression with embryonic MyHC, and immunostaining was coexpressed with this isoform (Fig. 6). There was a 100% overlap between myofibers positive for embryonic MyHC isoform and WDFY1.

Ingenuity Pathway Analysis

Differentially expressed genes were analyzed for significant differences in pathways and functions between the C57BL/6 and B6 albino mouse tissues (Fig. 7). Other differences between the EOM of each genotype and for both EOM and

Investigative Ophthalmology & Visual Science

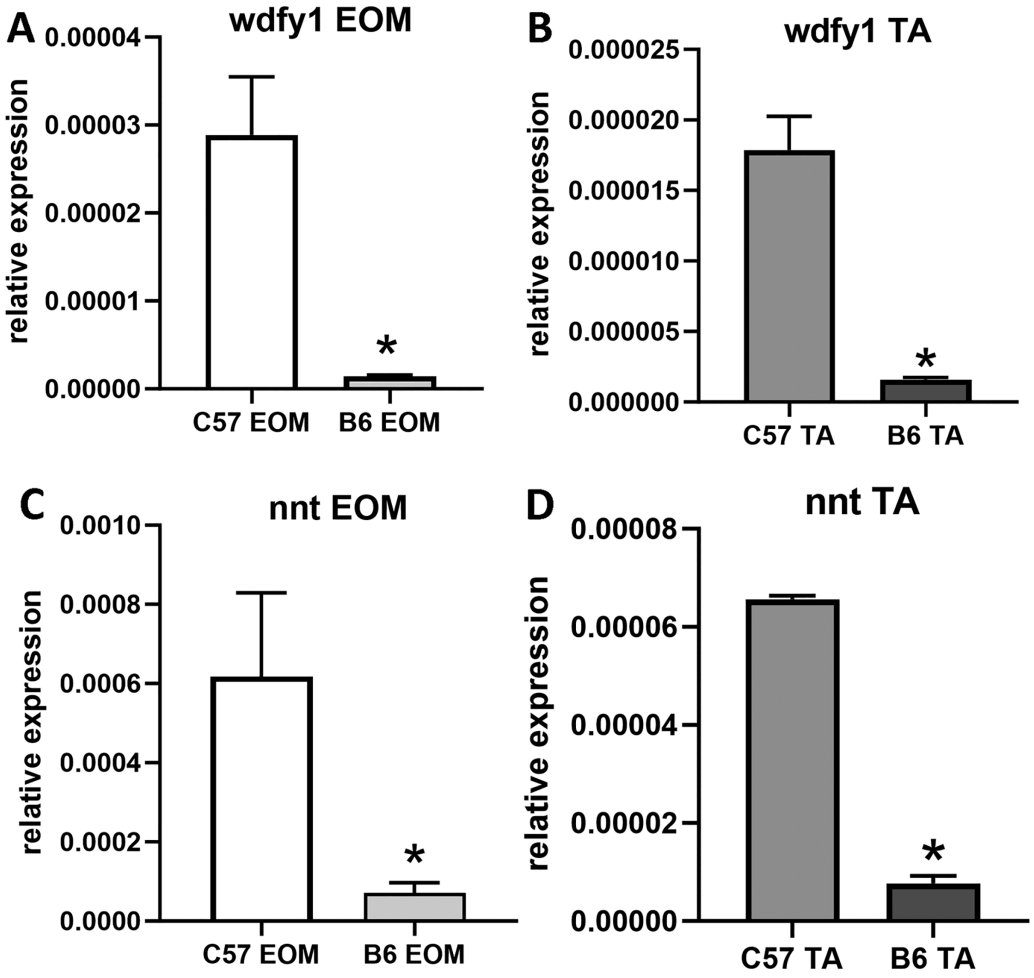

Figure 5. The qPCR analysis for (**A**, **B**) *wdfy1* and (**C**, **D**) *nnt* as a ratio of GAPDH expression. These validate the RNA-Seq analysis, showing reduced expression in the B6 albino tissues compared to the C57BL/6 mouse. *Asterisk* indicates significant difference from wt controls of the same tissue.

TA include axonal guidance signaling and neuromuscular junction formation.

The top physiological and disease related pathways were examined between the C57BL/6 and the B6 albinos and a large number of significant differences were seen in similar pathways for all tissues examined (Figs. 8, 9). These include those specifically associated with muscle: cardiovascular system development and function and skeletal and muscular system development and function, and include genes such as dystrophin, IGF1, and serpine1. Additionally in the EOM, there are significant decreases in MyHC for fast 2X and 2B fibers in the B6 albino muscles (data not shown). Differences in expression of fast IIA myofibers were further demonstrated using immunohistochemistry (Fig. 10). There were significantly fewer WDFY1-positive myofibers in the EOM from the B6 albino mice (Figs. 10G, 10H), with 42.8% fewer WDFY1-positive fibers in the B6 albino EOM ($P = 0.0003$). In addition, there were 72.2% fewer double positive fibers in the B6 albino EOM ($P = 0.0003$) compared to the WT controls.

Discussion

Mice with a mutation in the tyrosinase gene, the B6(CG)-Tyr(c-2J)/J (B6 albino) mouse, which is otherwise identical genetically to a C57BL/6 mouse, all exhibited waveforms consistent with nystagmus—defined as uncontrolled oscillatory movements of the eyes both in the absence of stimulation and in the presence of the horizontally moving black and white bars used to test OKR.[14] A previous study examined a number of albino mouse strains, CD1, BALB/c and DBA/1, and using OKR eye tracking showed nystagmus phenotypes compared to pigmented controls.[5] Thus we had hypothesized that, despite the C57BL/6 background, the B6 albino mice would have nystagmus. Although Traber et al.[5] did not explicitly state the mice were dark adapted, they do say they did all their testing in a dark room. In the B6 albino mice, to demonstrate a response with the OKR stimulus, they had to be dark adapted. Other studies examining the OKR in albino mice that were not dark adapted have reported the absence of eye movements in the presence of stimulation in CD1[8], BALB/c[9], and DBA2[9,10] albino mice, despite the presence of normal structure and function of the retina itself.[9] Based on the presence of uncontrolled oscillatory movements, we performed a transcriptome analysis between these two mouse strains with only one genetic mutation between the two genotypes.

Typically, the cause of nystagmus is described as a disturbance in the central nervous system oculomotor control pathways.[15,16] Changes to the visual pathway such as foveal

Investigative Ophthalmology & Visual Science

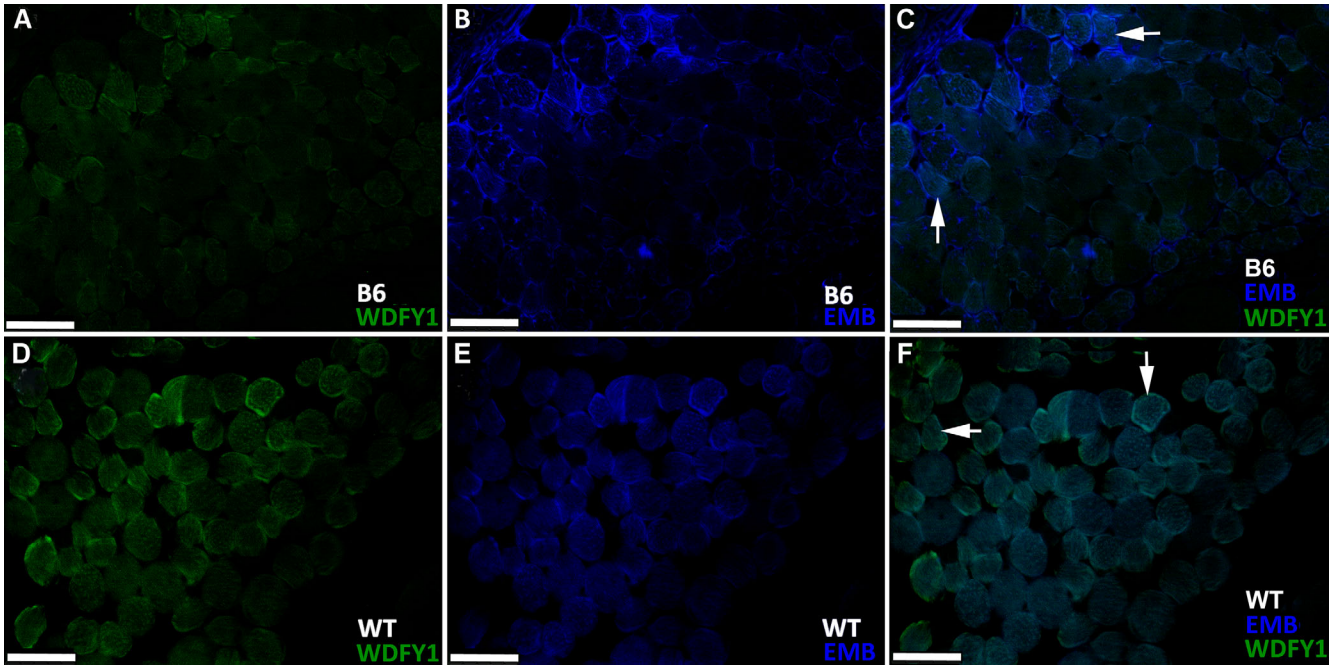

Figure 6. Immunofluorescent staining of (**A–C**) B6 albino extraocular muscle and (**D–F**) control (WT) extraocular muscle for (**A**, **C**, **D**, **F**) WDFY1 (*green*) and (**B**, **C**, **E**, **F**) embryonic myosin heavy chain isoform. WDFY1 is down-regulated in the B6 albino extraocular muscle compared to the control C57BL/6 muscles, and almost 100% of the WDFY1-positive fibers also express the embryonic myosin heavy chain isoform. Arrows indicate examples of myofibers coexpressing these two proteins. *Scale bar:* 50 µm.

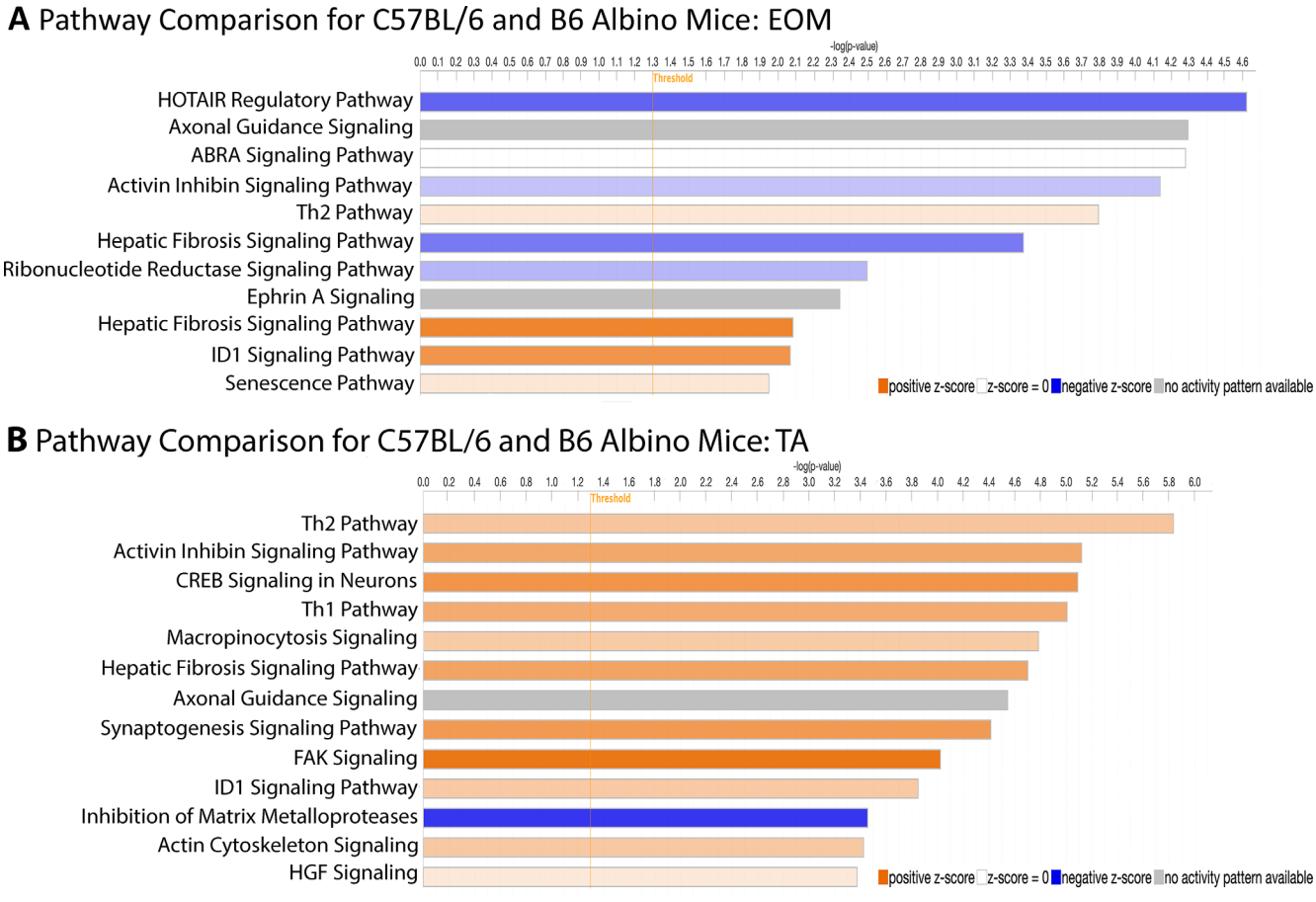

Figure 7. Top differentially expressed cellular growth, proliferation and development, organismal growth and development pathways for (**A**) EOM and (**B**) TA. X-axis is −log (*P* value) with the threshold set at $P < 0.05$. Each bar is colored according to its predicted activation or inactivation. *Orange* is predicted increased activation; *blue* is predicted decreased activation. Darker colors indicate higher absolute z-scores.

Investigative Ophthalmology & Visual Science

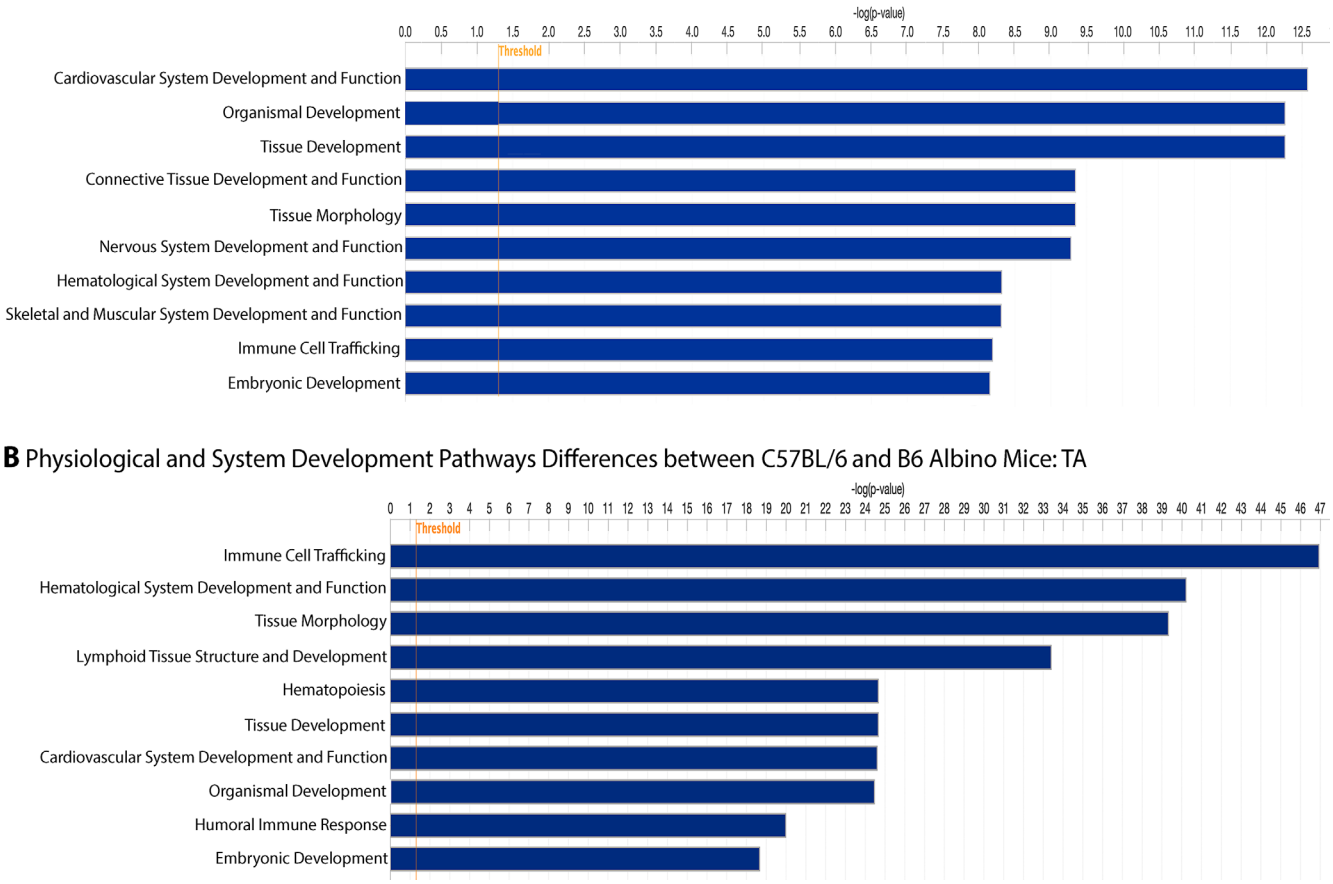

Figure 8. Top ten differentially expressed physiological system development and function pathways for (**A**) EOM and (**B**) TA. X-axis is −log (*P* value) with the threshold set at *P* value < 0.05.

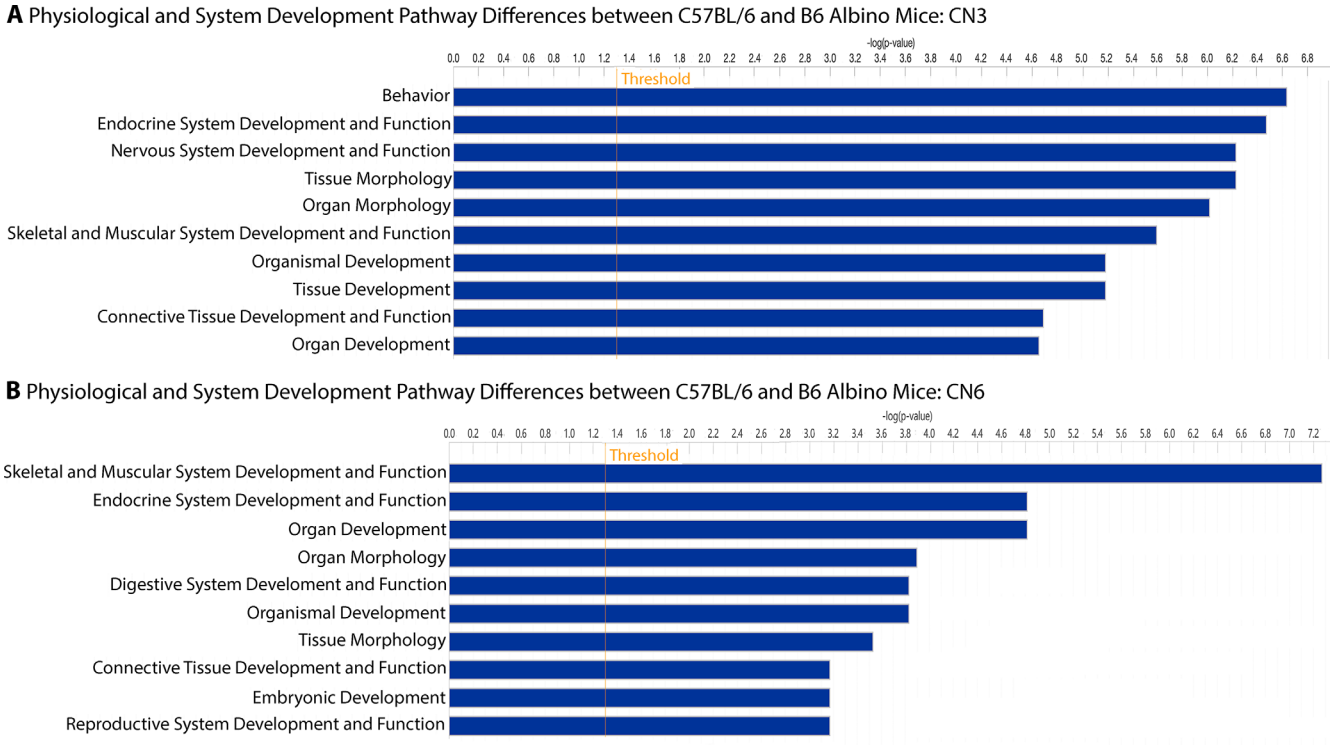

Figure 9. Top ten differentially expressed physiological system development and function pathways for (**A**) CN3 and (**B**) CN6. X-axis is −log (*P* value) with the threshold set at *P* value < 0.05.

Investigative Ophthalmology & Visual Science

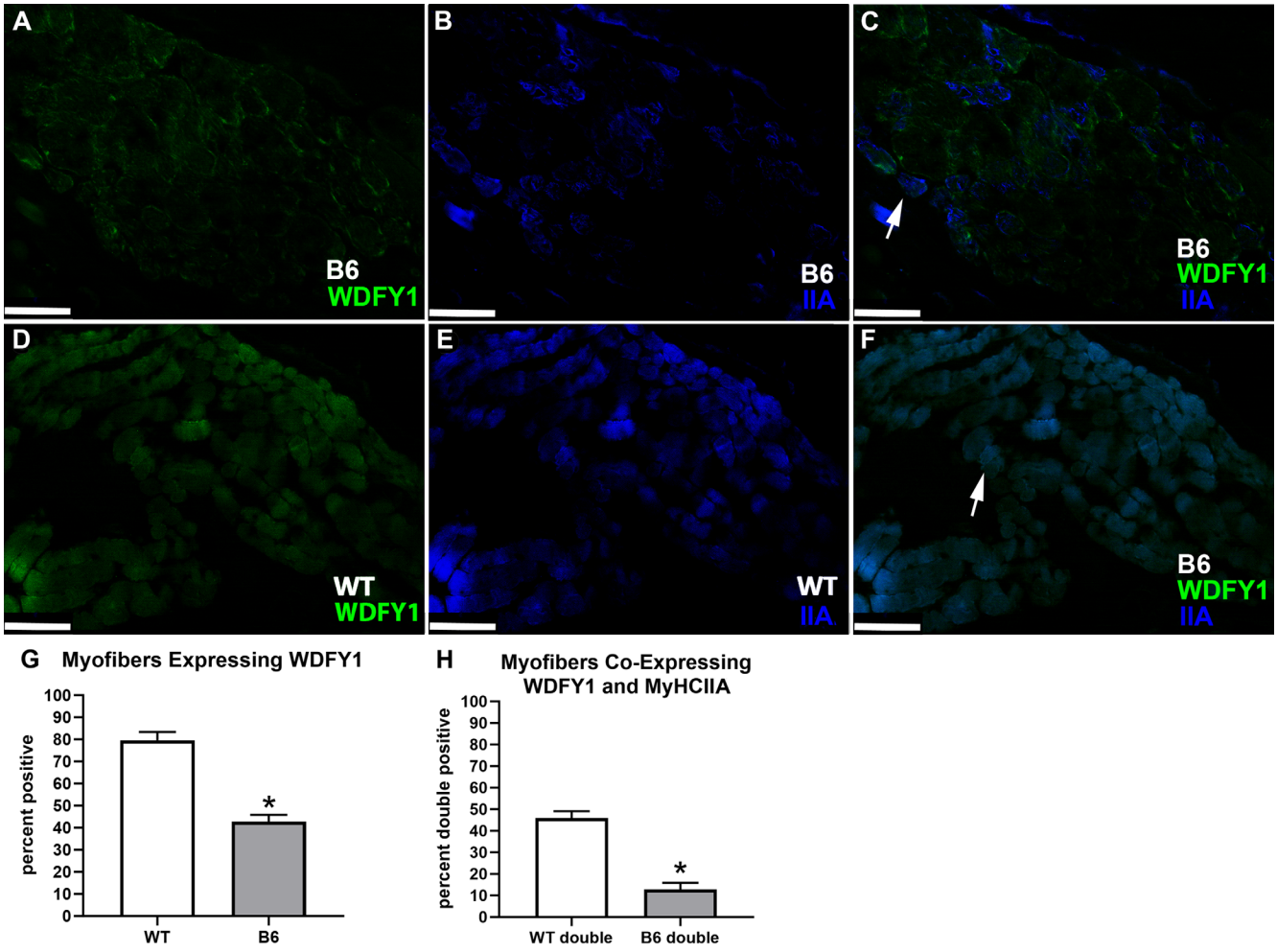

Figure 10. Immunofluorescent staining of (**A–C**) B6 albino extraocular muscle and (**D–F**) control (WT) extraocular muscle for (**A**, **C**, **D**, **F**) WDFY1 (*green*) and (**B**, **C**, **E**, **F**) type IIA myosin heavy chain isoform. This further validates that WDFY1 appears to have reduced expression levels in the B6 albino extraocular muscle compared to the control C57BL/6 muscles. (**G**) Percent of myofibers expressing WDFY1 and (**H**) coexpressing both WDFY1 and type IIA MyHC were determined. *Arrows* indicate examples of myofibers coexpressing these two proteins. *Scale bar* for **A–C**: 50 µm; *scale bar* for **D–F**: 75 µm. *Asterisk* indicates significantly different from control muscles.

hypoplasia, optic nerve hypoplasia, and achiasma are all associated with nystagmus, along with albinism.[4] Oculocutaneous albinism is characterized by a lack of pigment in the eyes, skin, and hair due to a disruption in the production of melanin. This disruption in the production of melanin can come from multiple genes, including *OCA1/2/3/4, TYR, TYRP1*, and *MATP*.[3] To simplify this study we used the tyrosinase gene, *tyr*, and a mouse with a mutation solely in this gene (JAX stock no. 000058)[6] to produce a phenotypically albino mouse on a normal C57BL/6 mouse background. The normal C57BL/6 mouse without the *tyr* mutation is phenotypically pigmented and has normal eye movements during OKR. The B6 albino mice had waveforms typical of nystagmus, both in the dark and in the presence of the OKR stimulus. It should also be noted that the variability in waveforms is often seen in children with nystagmus,[14] and generally there is not a clear relationship between waveform characteristics and specific clinical conditions.

Transcriptome analysis of this mouse strain compared to the control mice through RNA-Seq showed quality data across all of the tissue types (EOM, TA, CN3, and CN6). Typically, when looking at quality RNA-Seq experiments, a PCA plot or a heat map showing how all of the samples are similar to each other through distance matrices will show clusters by similar samples. In this study's case there is clustering of samples by tissue type with respect to muscle compared to cranial neurons as the main principal component, then a second principal component making the muscle cluster break into EOM compared to TA but not breaking up the cranial motor neuron cluster. We hypothesize that this tight clustering of the RNA expression patterns in the cranial motor neurons compared to the muscles is due to the EOM being developmentally different than other limb and skeletal muscles of the body,[17–19] such as the TA muscle, whereas the motor neurons innervating the EOM are more similar to each other molecularly.

RNA-Seq data used to analyze the transcriptome of the EOM, the TA, the cranial oculomotor neuronal pool, and the abducens motor neuronal pool in the C57BL/6 mouse and the B6 albino mouse revealed multiple differentially expressed genes overlapping between each tissue. These genes can be used for further studies on their potential role in nystagmus. Two genes, *wdfy1* and *nnt*, were differentially expressed in all four tissue types between the C57BL/6

Investigative Ophthalmology & Visual Science

mice and the B6 albino mice. *Wdfy1* codes for a protein localized to early endosomes after forming a complex that recognizes damaged lysosomes.[20,21] *Nnt* codes for nicotinamide nucleotide transhydrogenase, an integral protein for proton translocation across the inner mitochondrial membrane[22] and has been implicated in mitochondrial dysfunction[23] and in maintenance of stem cells in other systems.[24,25] However, the role and function of *wdfy1* and *nnt* in the EOM or nystagmus has not been studied previously. The decrease in gene expression between the B6 albino to the C57BL/6 for both of these genes, *wdfy1* and *nnt*, was confirmed using qPCR and immunochemistry.

Nystagmus in humans is routinely associated with central nervous system oculomotor control pathway abnormalities. Pathway analysis using IPA for the EOM and TA revealed differences between the C57BL/6 and the B6 albino mice in axonal guidance signaling. Differences in physiological and system development between the C57BL/6 and B6 albino mice in the CN3 and CN6 include pathways in both skeletal and muscular system development and function. These differences suggest adaptations that resulted in changes in axonal guidance in the development of the CN3 and CN6 nerves, as well as the muscles they innervate. The genes associated with these adaptations may provide potential candidates for manipulation with the hope of altering nystagmus at the genetic or pathway level.

Furthermore, there were 11 genes differentially expressed in the CN3 and CN6, 3 genes differentially expressed in both the EOM and CN3. 286 genes were differentially expressed only in the EOM, 7 only in CN6, and 49 only in CN3. The genes that are differentially expressed in the tissues associated with the EOM, CN3 and CN6, could show important RNA level differences between the C57BL/6 mice and the B6 albino mice with respect to nystagmus. Changes in percent of myofibers expressing the fast myosin heavy chain isoforms would have a significant effect on muscle shortening velocity.[26] It should be noted that these differences are likely to be compensatory to the primary cause of the nystagmus, although it has been shown that innervational differences in adult albino mice[27] are present before eye opening.[28]

Differentially expressed genes were analyzed for significant differences in pathways and functions between the C57BL/6 and B6 albino mouse tissues. For example, in the EOM, pathway analysis showed significant downregulation of the HOTAIR regulatory pathway. HOTAIR is a long noncoding RNA that plays a role in myogenic cell proliferation, and decreases can result in decreased proliferation.[29,30] Other differences between the EOM of each genotype and for both EOM and TA include axonal guidance signaling. This included decreases in the B6 albino tissues of molecules known to be expressed in muscle, synapses, and axon pathfinding to include the ephrin receptor A3, semaphorin 3A, D, and E, the MET receptor, and IGF1. Because we have previously demonstrated decreased axon density and neuromuscular junction size in human EOM from individuals with albinism, this suggests possible downstream molecules that might be amenable for focusing new therapeutic approaches.

In summary, we have demonstrated that the *tyr* gene mutation is sufficient in this mouse model to result in nystagmus. RNA-seq analysis of the EOM, and cranial motor neurons from oculomotor and abducens nuclei identified two genes whose expression was significantly decreased in all these tissues from the B6 albino mice: *wdfy1* and *nnt*. Their potential role in the etiology and/or maintenance of nystagmus is the subject of ongoing investigation. These genes implicate a potential mitochondrial basis for some forms of INS. Other genes identified in these studies may also play a compensatory role in maintaining nystagmus and thus have potential for the modification of nystagmus.

Acknowledgments

Supported by EY15313 (LKM) and P30 EY11375 and from the National Eye Institute, and the Minnesota Lions Foundation.

Disclosure: **L.L. Johnson**, None; **J.E. Abrahante**, None; **L.K. McLoon**, None

References

1. Sarvananthan N, Surendran M, Roberts EO, et al. The prevalence of nystagmus: the Leicestershire nystagmus survey. *Invest Ophthalmol Vis Sci*. 2009;50:5201–5206.
2. Collewijn H, Apkarian P, Spekreijse H. The oculomotor behavior of human albinos. *Brain*. 1985;108:1–18.
3. Abadi RV, Bjerre A. Motor and sensory characteristics of infantile nystagmus. *Br J Ophthalmol*. 2002;86:1152–1160.
4. Grønskov K, Ek J, Brondum-Nielsen K. Oculocutaneous albinism. *Orphanet J Rare Dis*. 2007;2:43.
5. Traber GL, Chen CC, Huang YY, et al. Albino mice as an animal model for infantile nystagmus syndrome. *Invest Ophthalmol Vis Sci*. 2012;53:5737–5747.
6. Townsend D, Witkop CJ, Jr., Mattson J. Tyrosinase subcellular distribution and kinetic parameters in wild type and c-locus mutant C57BL/6J mice. *J Exp Zool*. 1981:216:113–119.
7. Johnson LL, Kueppers RB, Shen EY, Rudell JC, McLoon LK. Development of nystagmus with the absence of MYOD expression in the extraocular muscles. *Invest Ophthalmol Vis Sci*. 2021;62(13):3.
8. Abdeljalil J, Hamid M, Abdel-mouttalib O, et al. The optomotor response: a robust first-line visual screening method for mice. *Vis Res*. 2005;45:1439–1446.
9. Puk O, Dalke C, Hrabe de Angelis M, Graw J. Variation of the response to the optokinetic drum among various strains of mice. *Front Biosci*. 2008;13:6269–6275.
10. Barabas P, Huang W, Chen H., et al. Missing optomotor head-turning reflex in the DBA/2J mouse. *Invest Ophthalmol Vis Sci*. 2011;52:6766–6773.
11. Van Alphen B, Winkelman BHJ, Frens MA. Three-dimensional optokinetic eye movements in the C57BL/6J mouse. *Invest Ophthalmol Vis Sci*. 2010;51:623–630.
12. Dell'Osso LF, Daroff RB. Congenital nystagmus waveforms and foveation strategy. *Doc Ophthalmol*. 1975;39:155–182.
13. Oliveros JC. (2007-2015) Venny. An interactive tool for comparing lists with Venn's diagrams. Available at: https://bioinfogp.cnb.csic.es/tools/venny/index.html. Accessed 2020–2023.
14. Hertle RW, Dell'Osso LF. Clinical and ocular motor analysis of congenital nystagmus in infancy. *J AAPOS*. 1999:3:70–79.
15. Bertsch M, Floyd M, Kehoe T, Pfeifer W, Drack AV. The clinical evaluation of infantile nystagmus: what to do first and why. *Ophthalmic Genet*. 2017;38(1):22–33.
16. Peragallo JH. Effects of brain tumors on vision in children. *Int Ophthalmol Clin*. 2018;58(4):83–95.
17. Tajbakhsh S, Rocancourt D, Cossu G, Buckingham M. Redefining the genetic hierarchies controlling skeletal myogenesis: pax-3 and Myf-5 act upstream of MyoD. *Cell*. 1997;89(1):127–138.

18. Kitamura K., Miura H, Miyagawa-Tomita S, et al. Mouse Pitx2 deficiency leads to anomalies of the ventral body wall, heart, extra- and periocular mesoderm and right pulmonary isomerism. *Development*. 1999;126:5749–5758.
19. Diehl AG, Zareparsi S, Qian M, Khanna R, Angeles R, Gage PJ. Extraocular muscle morphogenesis and gene expression are regulated by Pitx2 gene dose. *Invest Ophthalmol Vis Sci*. 2006;47:1785–1793.
20. Teranishi H, Tabata K, Saeki M, et al. Identification of CUL4A-DDB1-WDFY1 as an E3 ubiquitin ligase complex involved in initiation of lysophagy. *Cell Rep*. 2022;40(11):111349.
21. Ridley SH, Ktistakis N, Davidson K, et al. FENS-1 and DFCP1 are FYVE domain-containing proteins with distinct functions in the endosomal and Golgi compartments. *J Cell Sci*. 2001;114:3991–4000.
22. Hoek JB, Rydström J. Physiological roles of nicotinamide nucleotide transhydrogenase. *Biochem J*. 1988;254:1–10.
23. Rydström J. Mitochondrial NADPH, transhydrogenase, and disease. *Biochim Biophys Acta*. 2006;1757:721–726.
24. Son MJ, Kwon Y, Son T, Cho YS. Restoration of mitochondrial NAD+ levels delays stem cell senescence and facilitates reprogramming of aged somatic cells. *Stem Cells*. 2016;34:2840–2851.
25. Seo BJ, Yoon SH, Do JT. Mitochondrial dynamics in stem cells and differentiation. *Int J Mol Sci*. 2018;19:3893.
26. Larsson L, Li X, Frontera WR. Effect of aging on shortening velocity and myosin isoform composition in single human skeletal muscle cells. *Am J Physiol*. 1997;272(Pt1):C638–C649.
27. McLoon LK, Willoughby CL, Anderson JS, et al. Abnormally small neuromuscular junctions in the extraocular muscles from subjects with idiopathic nystagmus and nystagmus-associated with albinism. *Invest Ophthalmol Vis Sci*. 2016;57:1912–1920.
28. Vemela SK, Kim SA, Muvavariwa T, Bell JL, Whitman MC. Impaired extraocular muscle innervation is present before eye opening in a mouse model of infantile nystagmus syndrome. *Invest Ophthalmol Vis Sci*. 2022;63(10):4.
29. Wang S, Jin J, Xu Z, Zuo B. Functions and regulatory mechanisms of lncRNAs in skeletal myogenesis, muscle disease, and meat production. *Cells*. 2019;8:1107.
30. Hu CY, Su BH, Lee YC, et al. Interruption of the long non-coding RNA HOTAIR signaling axis ameliorates chemotherapy-induced cachexia in bladder cancer. *J Biomed Sci*. 2022;29:104.

Investigative Ophthalmology & Visual Science